

AD-A119 172 AIR WEATHER SERVICE SCOTT AFB IL F/8 4/2
THE PLATTEVILLE RADAR PROFILER AS A METEOROLOGICAL AND COMMUNIC--ETC(U)
JAN 82 G O NASTROM
UNCLASSIFIED ANS/TN-82/003 SBI-AD-E850 178 NL

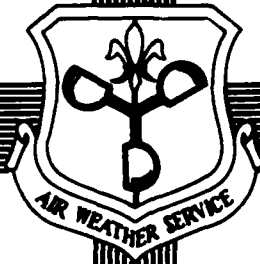
END
DATE
FORM
11-80

ADE 850 172

AWS/TN-82/003

(2)

AD A119172



THE PLATTEVILLE RADAR PROFILER AS A
METEOROLOGICAL AND COMMUNICATIONS
ENGINEERING TOOL

BY

GREGORY D. NASTROM, CAPT, USAFR

JANUARY 1982

DTIC
ELECTRONIC
SEP 10 1982
A

DTIC FILE COPY

Approved For Public Release; Distribution Unlimited


AIR WEATHER SERVICE (MAC)
Scott AFB, Illinois 62225

88 07 87 074

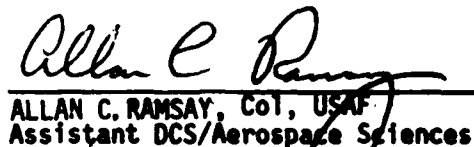
REVIEW AND APPROVAL STATEMENT

AWS/TN-82/003, The Platteville Radar Profiler as a Meteorological and Communications Engineering Tool, January 1982, is approved for public release. There is no objection to unlimited distribution of this document to the public at large, or by the Defense Technical Information Center (DTIC) to the National Technical Information Service (NTIS).

This Technical Note has been reviewed and is approved for publication.


JOHN S. BOHLSON, LtCol, USAF
Chief, Directorate of Aerospace Services
Reviewing Officer

FOR THE COMMANDER


ALLAN C. RAMSAY, Col, USAF
Assistant DCS/Aerospace Sciences

UNCLASSIFIED

SECURITY CLASSIFICATION OF THIS PAGE (When Data Entered)

REPORT DOCUMENTATION PAGE		READ INSTRUCTIONS BEFORE COMPLETING FORM
1. REPORT NUMBER AWS/TN-82/003	2. GOVT ACCESSION NO. AD-A119172	3. RECIPIENT'S CATALOG NUMBER
4. TITLE (and Subtitle) The Platteville Radar Profiler as a Meteorological and Communications Engineering Tool		5. TYPE OF REPORT & PERIOD COVERED Technical Note
7. AUTHOR(s) Gregory D. Nastrom, Capt, USAFR		6. PERFORMING ORG. REPORT NUMBER
9. PERFORMING ORGANIZATION NAME AND ADDRESS Headquarters Air Weather Service/IN Scott Air Force Base, Illinois 62225		8. CONTRACT OR GRANT NUMBER(s)
11. CONTROLLING OFFICE NAME AND ADDRESS Headquarters Air Weather Service Scott Air Force Base, Illinois 62225		10. PROGRAM ELEMENT, PROJECT, TASK AREA & WORK UNIT NUMBERS
14. MONITORING AGENCY NAME & ADDRESS (if different from Controlling Office)		12. REPORT DATE JANUARY 1982
		13. NUMBER OF PAGES 16
		15. SECURITY CLASS. (of this report) Unclassified
		16a. DECLASSIFICATION/DOWNGRADING SCHEDULE
16. DISTRIBUTION STATEMENT (of this Report) Approved for public release; distribution unlimited		
17. DISTRIBUTION STATEMENT (of the abstract entered in Block 20, if different from Report)		
18. SUPPLEMENTARY NOTES		
19. KEY WORDS (Continue on reverse side if necessary and identify by block number) Stratosphere Troposphere Radar, Atmospheric Turbulence, Atmospheric Sounding, Platteville Radar, Wind Sounding, Temperature Sounding, Meteorology Colorado, Platteville, *stratosphere, *Doppler Radar Meteorological Radar		
20. ABSTRACT (Continue on reverse side if necessary and identify by block number) The basic operating principles and capabilities of the VHF pulsed Doppler radar located at Platteville, Colorado, are discussed. Examples of horizontal and vertical wind speed measurements are presented, and the meteorological uses of these data are briefly outlined. The radar backscattered power is used to compute the refractivity turbulence structure constant. New results on the variability of the refractivity turbulence structure constant from about 5-15 km are given. Especially interesting is the large diurnal change of the constant in the upper atmosphere.		

DD FORM 1 JAN 73 1473

EDITION OF 1 NOV 68 IS OBSOLETE



Accession For	
DTIC	<input checked="" type="checkbox"/>
ISB	<input type="checkbox"/>
Unneeded	<input type="checkbox"/>
Distribution/	
Availability Codes	
and, or	
1st	
2nd	
3rd	
4th	
5th	
6th	
7th	
8th	
9th	
10th	
11th	
12th	
13th	
14th	
15th	
16th	
17th	
18th	
19th	
20th	
21st	
22nd	
23rd	
24th	
25th	
26th	
27th	
28th	
29th	
30th	
31st	
32nd	
33rd	
34th	
35th	
36th	
37th	
38th	
39th	
40th	
41st	
42nd	
43rd	
44th	
45th	
46th	
47th	
48th	
49th	
50th	
51st	
52nd	
53rd	
54th	
55th	
56th	
57th	
58th	
59th	
60th	
61st	
62nd	
63rd	
64th	
65th	
66th	
67th	
68th	
69th	
70th	
71st	
72nd	
73rd	
74th	
75th	
76th	
77th	
78th	
79th	
80th	
81st	
82nd	
83rd	
84th	
85th	
86th	
87th	
88th	
89th	
90th	
91st	
92nd	
93rd	
94th	
95th	
96th	
97th	
98th	
99th	
100th	

TABLE OF CONTENTS

	Page
Introduction.	1
Meteorological Applications	1
Applications to Communications Systems.	4
Data Analysis	6
Summary and Conclusions	11
Acknowledgement	12
References.	12

ILLUSTRATIONS

Figure 1. Sample Doppler spectrum from Platteville ST radar, east receiver at 9.5 km for 1548 MST, May 7, 1981.	2
Figure 2. Horizontal wind vectors at Platteville	3
Figure 3. Vertical wind velocities at Platteville.	5
Figure 4. Time series of $\log C_n^2$ at 5.3 km at Platteville for both antenna systems.	7
Figure 5. Vertical profiles of mean C_n^2 at Platteville for both antenna systems	7
Figure 6. Probability density functions of half-hour averages of C_n^2 by altitude.	8
Figure 7. Diurnal variation of C_n^2 at Platteville by altitude	9
Figure 8. Vertical profiles of diurnal range (max/min) and time of maximum of C_n^2	10
Figure 9. Probability density functions for night- and daytime hours	10
Figure 10. Time series of $\log C_n^2$ and wind speed at 8.2 km	11

TABLES

Table 1. Platteville Radar Parameters.	1
Table 2. Platteville Radar Data Used for Study for C_n^2	6

The Platteville Radar Profiler as a Meteorological
and Communications Engineering Tool

by

Gregory D. Nastrom, Capt, USAFR

1. Introduction

The term wind "profiler" has gained wide usage in the Prototype Regional Observing and Forecasting Service (PROFS) community to refer to the Very High Frequency (VHF) pulsed Doppler radar located near Platteville, CO. This radar was constructed in 1978 (1) and is a ST, or MST, radar (for Mesosphere-Stratosphere-Troposphere). The many potential users of ST radars for studies of atmospheric structure and dynamics are discussed in recent review articles. The purpose of this technical note is to present examples of results from the Platteville radar data which apply to two important military problem areas: meteorology and communications.

As the name "profiler" implies, the intended purpose of this radar within PROFS has been to monitor the wind profiles. While useful studies have been made using the radar data alone (2, 3), the most fruitful results from these high time resolution wind profiles will come when they are combined with other meso- and micro-scale meteorological programs such as PROFS.

A less widely appreciated use of the radar data is to study a parameter related to the scattering of radio waves, the refractivity, turbulence structure constant, C_n^2 . This technical note outlines the rationale for obtaining C_n^2 from the radar data and presents climatological results obtained using data from April and early May, 1981. Vertical profiles of C_n^2 from 3-16 km are given, and its variability with changing wind speed and time of day is studied. Finally, C_n^2 is related to the meteorological variable ϵ , the eddy dissipation rate, which implies that the variations found in C_n^2 may have meteorological consequences.

2. Meteorological Applications

The ST radar at Platteville is a phased dipole array, using three antennas to measure the three components of the wind (1, 4). Two of the antennas are superposed, pointing 15 degrees off vertical toward the north and toward the east, and the antenna which is used to measure vertical winds is directed toward the zenith. Normal operating parameters are listed in Table 1.

Table 1. Platteville Radar Parameters

A	Antenna area	10^4 m^2
	Antenna efficiency	0.3
F	radar frequency	49.9 MHz
λ	wavelength	6.01 m
pw	pulse width	16 μs
τ	interpulse period	2400 μs
P_t	peak pulse power	360 w
N_c	number of spectra	32
	coherently averaged	
Δr	range spacing	1500 m
χ	zenith angle east antenna	15°
	zenith angle north antenna	15°
	zenith angle vertical antenna	0

The atmospheric echoes observed by the ST radar arise from the scattering of radar waves by irregularities in the radio refractive index with scale sizes comparable to one-half the radar wavelengths (5). It is usually assumed that these irregularities (three-meter scale for the Platteville radar) are due to homogeneous, isotropic turbulence. Another assumption often used is that the three-meter scale size lies within the inertial subrange (6). Because the irregularities are advected with the background wind, the measured radial wind speed is directly related to the Doppler shift of the backscattered signal. If the vertical winds are assumed to be negligible, then the radial winds can be converted to horizontal winds. A typical example of a Doppler spectrum is given in Figure 1.

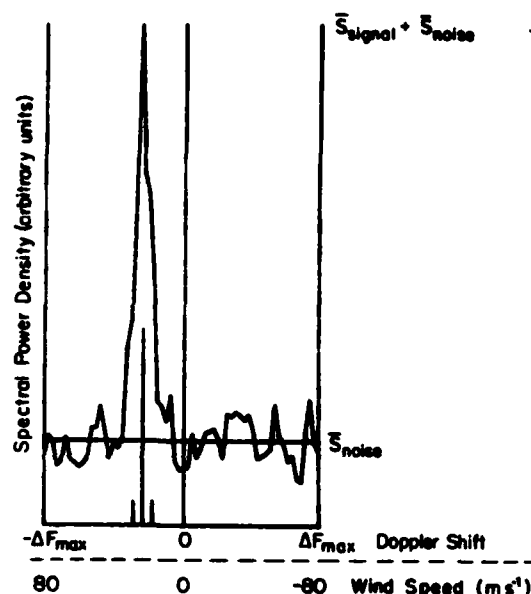


Figure 1. Sample Doppler spectrum from Platteville ST radar, east receiver at 9.5 km for 1548 MST, May 7, 1981.

In Figure 1, the peak backscattered power occurs at a frequency lower than the frequency transmitted (i.e., the peak has a negative Doppler shift). Since this antenna is pointed toward the east, we interpret this result to mean that the wind is moving toward the east, and that the wind speed is given by the magnitude of the Doppler shift. Small irregularities, or noise, are apparent to the left and right of the peak. While the data in Figure 1 are referred to as a single observation, they represent a time-average result obtained over several minutes. First, the sampled frequencies from 32 separate pulses are combined to give a single spectrum. This process is called coherent averaging. Next, 16 of these separate spectra are averaged to give an "archive observation", such as that in Figure 1. The purpose of all this averaging is to enhance the signal-to-noise ratio. The number of spectra averaged for each observation is determined by the time resolution desired between observations. For all data used in this note the basic time resolution is two and one-half minutes.

As with all radars, the time delay between transmission and reception determines the range (which can be converted to altitude) from which the echoes are received. Thus, by sampling at a series of time delays, winds at all heights can be measured, in principle. In practice, the backscattered signal decreases with increasing range so that at very large ranges it is not possible to distinguish the signal from the noise.

Samples of the horizontal winds measured at Platteville are given in Figure 2 for a very interesting period in February, 1981. These data are unedited, so occasional spurious echoes, which illustrate airplane reflections or other interference, are seen but should be disregarded. The growth of a southwesterly jet stream and subsequent passage of a trough axis near 0900 on February 21st are the most obvious features present. However, these features could have been detected with routine 12-hourly radiosonde data. Features uniquely evident from the high time resolution possible with an ST radar include the relative suddenness of the trough passage, the

wavelike changes in the wind near 7 km at 1800 MST on February 20th and the rapid changes of speed and direction near 6 km at 0200 MST, on February 20th. This illustrates that a great deal of the wind's variability is missed if one has only occasional balloon flights.

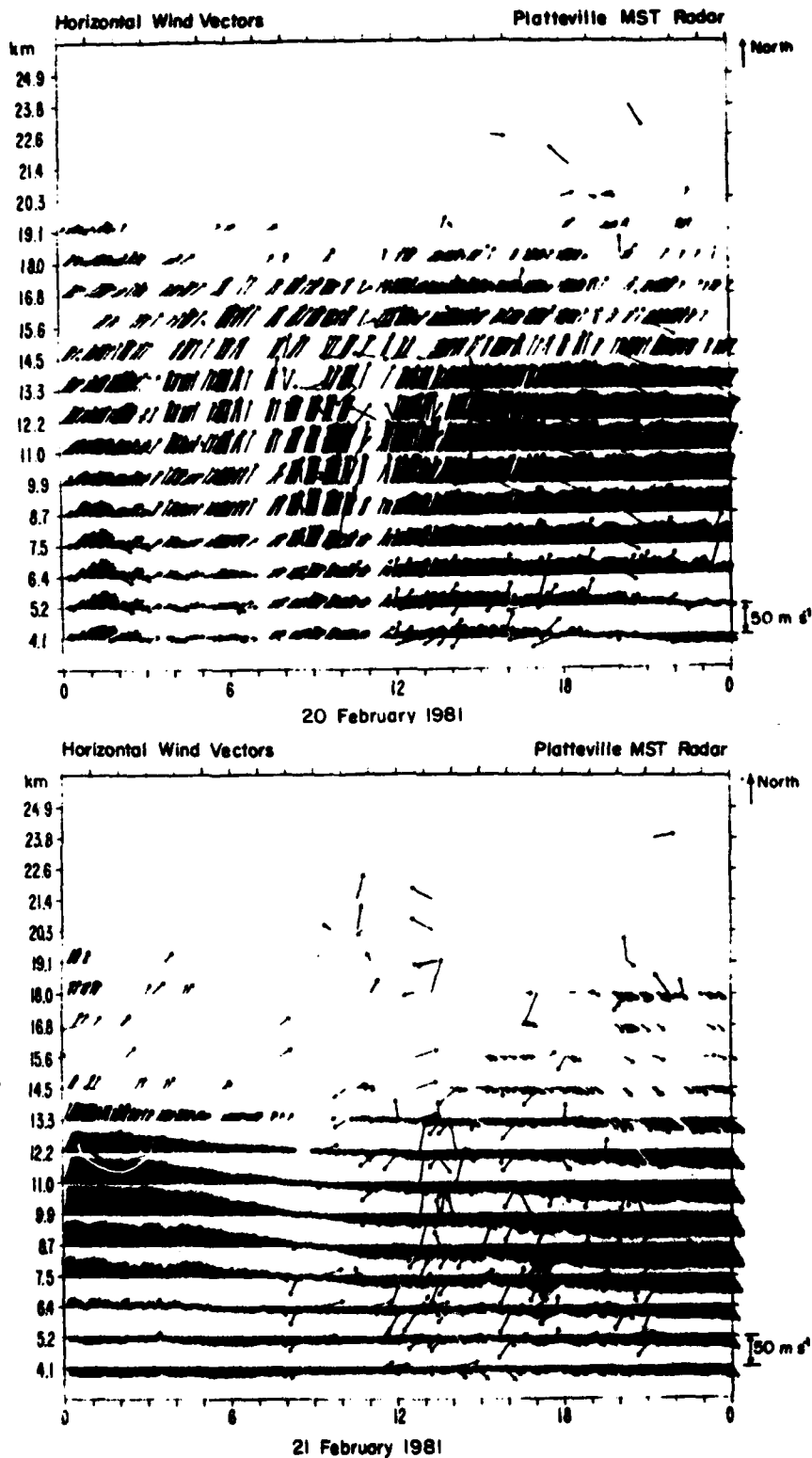


Figure 2. Horizontal wind vectors at Platteville. Basic time resolution is two and one half minutes.

The potential application of ST radar wind data for updating meteorological forecasts, for identifying areas of intense wind shears, as input in ballistics computations, or even as basic data for developing climatological statistics of wind variability are exciting. But the potential of these data goes beyond the practical applications just mentioned, and they should help in new ways to improve our physical and theoretical understanding of the atmosphere. For example, the wave motions noted on February 20th may be internal gravity waves. The study of these waves, which may sometimes effect a rapid flux of momentum over large distances, is a topic currently of great interest among meteorologists. Also, by comparing the observed radar winds with those expected from the geostrophic relation one could follow the development of the so-called ageostrophic wind. By relating this wind with, say, the morphology of gravity wave activity, we may reach a better understanding of the atmospheric adjustment processes and, implicitly, be able to make better forecast models.

Figure 3 shows several weeks of uninterrupted vertical wind observations spanning several alternating periods of large and small vertical wind variability. The episodes of large activity always correspond with jet stream/frontal passages (7). The wavelike character of the vertical winds is obvious in many cases, again reminiscent of gravity waves. Direct, routine observation of the vertical winds is a new and challenging capability. Most sensible weather, e.g., clouds and precipitation, is very closely related to the vertical motions of the atmosphere but has historically been studied in terms of the more easily measured horizontal air motions and temperature changes. With the advent of routine observation of the vertical wind it will be possible to finally verify the indirect theoretical methods now used to infer vertical motions. Further, together with horizontal wind and temperature observations, these data will permit direct calculation of vertical heat and momentum fluxes - key variables in the development of storms.

Comparison of Figures 2 and 3 shows that the vertical antenna is able to detect winds to higher altitudes than the oblique antenna systems. This is due to the added backscattered power from partial reflections (8, 9) for the vertical antenna system. The partial reflections, or specular reflections, are believed to result from the presence of horizontally stratified layers of refractivity structure in the atmosphere. The probability of such layers is greater in the stratosphere than in the troposphere, so the altitude where the backscattered power for the vertical antenna system increases suddenly corresponds with the tropopause, providing a new method of tropopause detection (3).

3. Applications to Communications Systems

Returning to Figure 1, the area under the peak of the returned signal (i.e., above the average noise level, S (noise), and below the signal curve) is proportional to the backscattered power. Because the backscattered power is related to the intensity of the turbulence in the volume illuminated by the radar beam, these data yield estimates of the refractivity turbulence structure constant, C_n^2 . The parameter C_n^2 is often used in discussions of the turbulent scattering of radio waves and has direct applications in radio communications such as troposcatter and line-of-sight microwave systems (10). For optical propagation the appropriate parameter is C_T^2 , which differs from C_n^2 primarily in that it represents fluctuations in the ambient temperature and does not depend on humidity while C_n^2 does (11). Above about the mid-troposphere, however, humidity effects are very small, so that measurements of C_n^2 and C_T^2 can be directly related. The theory relating C_n^2 to backscattered power has been given in detail elsewhere (6), so only an outline will be presented next.

The refractivity structure constant C_n^2 is defined by

$$\overline{[n(r_0 + r) - n(r_0)]^2} = C_n^2 r^{2/3} \quad (1)$$

where the overbar defines a special integration (averaging). This applies for stationary, locally homogeneous, isotropic turbulence in the inertial subrange, and where n is the radio index of refraction and r is a distance measured from r_0 . The radar equation for turbulent scattering relates the backscattered power, P_B , to the power transmitted, P_T , the volume reflectivity, n , the range (altitude) r , and various radar parameters, which may be considered constant for a given operating configuration, as

$$P_B = \text{const}_1 \frac{P_T n}{r^2} \quad (2)$$

The volume reflectivity is related to C_n^2 and the radar wavelength, λ , as

$$n = \text{const}_2 C_n^2 \lambda^{1/3} \quad (3)$$

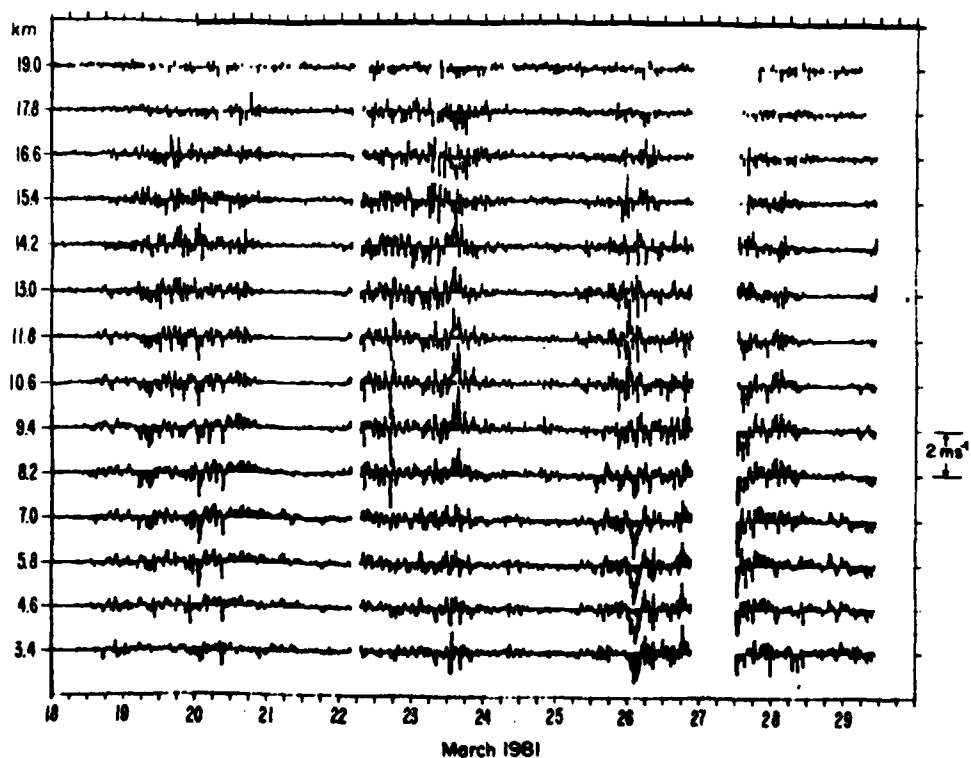
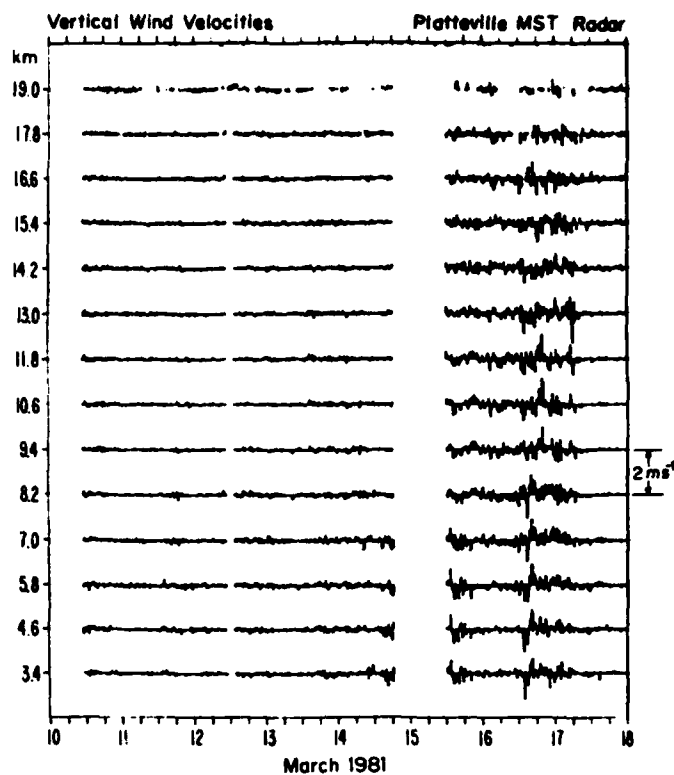


Figure 3. Vertical wind velocities at Platteville. Fifteen minute averages.

combining equations 2 and 3 we have

$$C_n^2 = \text{const}_3 \frac{P_B}{P_T} r^2 \quad (4)$$

The individual estimates of C_n^2 from Eq 4, are only accurate to about a factor to two, due to uncertainties in the radar operating parameters and in the measurement of P_B . However, since C_n^2 varies over several orders of magnitude, this uncertainty is relatively small.

Estimates of C_n^2 made using Eq 4 have been found to be consistent with those from other methods (6). There are only a few other ways to find C_n^2 in the remote atmosphere, such as optical scintillation observations of stars (12) or high response probes on balloons or airplanes (13), but these methods are restricted to nighttime, or are expensive to operate. Eq 4 can be used with ST radar data to provide reliable estimates of C_n^2 at many heights, around the clock, and over many days and in all weather.

4. Data Analysis

About eight days of data spread over a month period were available for the present study of C_n^2 (Table 2). A series of quality control algorithms, and hand editing, were used to discard those spectra contaminated by reflections from airplanes or which showed other problems. As C_n^2 sometimes changes by orders of magnitude in a fraction of an hour (b), the backscattered power values were averaged over half-hour intervals at each height to remove short period changes before applying Eq 4. All analyses were made separately for the east and north antenna systems.

Table 2. Platteville Radar Data Used for Study for C_n^2

Period	Number of Half-hour averages	Number of Observations	Denver Tropopause Height
7 Apr 1981/1530 - 8 Apr 1981/0930	34	376	11.6 km
13 Apr 1981/1300 - 15 Apr 1981/0100	66	732	11.8
16 Apr 1981/1000 - 17 Apr 1981/2230	72	763	12.2
7 May 1981/1500 - 9 May 1981/0230	64	805	9.6
	-----	-----	-----
Total/Average	236	2676	11.3

Sample time series of C_n^2 from the two antenna systems are given in Figure 4 and the mean vertical profiles for all available data are in Figure 5. The agreement among the mean vertical profiles is excellent. In Figure 4, the correlation of the data shown is 0.83, but if the single point at 1000 MST on April 17th were discarded, the correlation would be increased to nearly 0.9. The correlation is not expected to be perfect because the two antennas sample volumes of air which are a few km apart. The conclusion is that the two antenna systems give essentially the same results, so to save space only the curves for the north antenna will be included in the following figures.

The absolute values of C_n^2 in Figure 5 are similar to those found by others, i.e., the average decrease of about a factor of ten in five km (i.e., 2dB/km) between 5 and 15 km and the slight increase of C_n^2 just below the tropopause have been noted in data from other ST radars (6, 14). (The mean tropopause height during this period was 11.3 km from Table 2.) As the value of P_B , hence C_n^2 , at the lowest two heights is uncertain due to possible receiver gain delay problems, the dogleg at 5.3 km in Figure 5 may be an artifact of the data.

Hufnagel (15) and others have found that C_n^2 has a log-normal distribution, and this is verified in Figure 6 for the data from Platteville. The curves represent 236 half-hourly mean data points for the lower eight heights, and 206 data points at 15.5 km. In general the curves

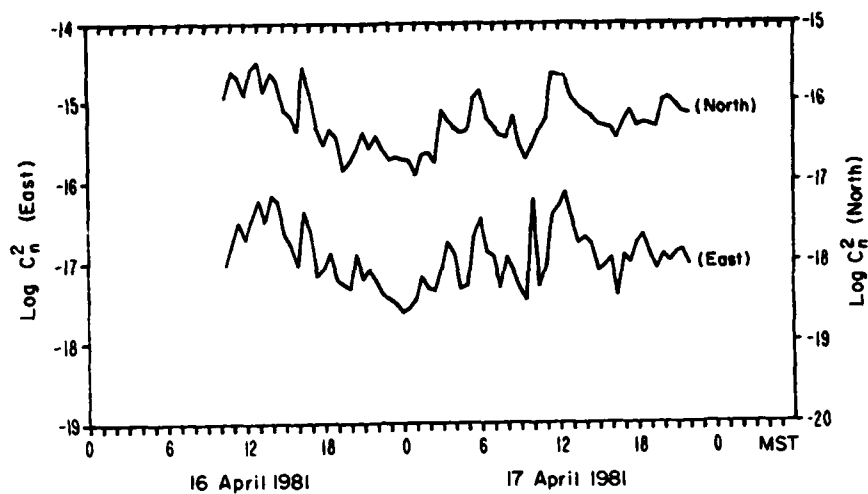


Figure 4. Time series of $\log C_n^2$ at 5.3 km at Platteville for both antenna systems. Half-hourly averages. correlation = 0.83.

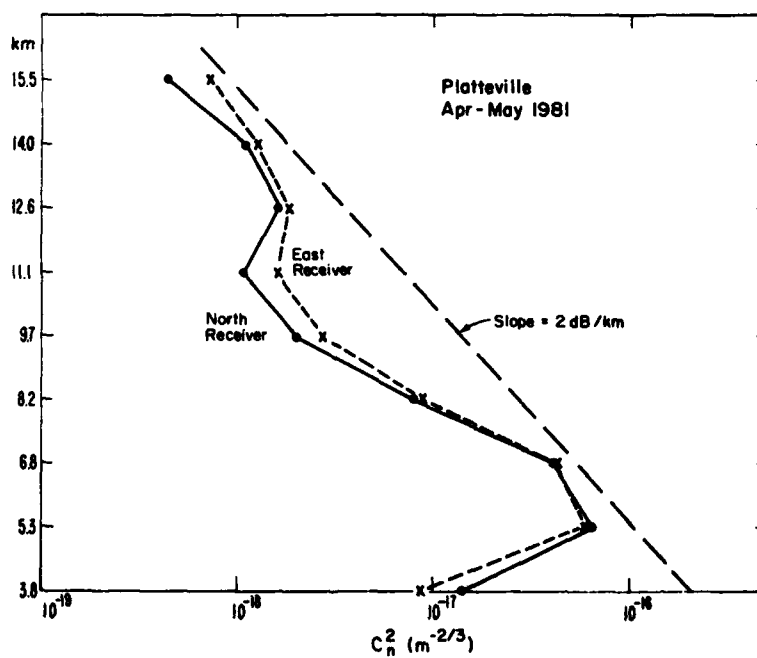


Figure 5. Vertical profiles of mean C_n^2 at Platteville for both antenna systems.

have the bell-shape characteristic of a normal distribution, and the mean and mode at each level agree closely. The long tail on the curve at 15.5 km shows that in some cases the signal-to-noise ratio here falls below the threshold of reliability. The standard deviation of the distribution in Figure 6 is about 4 dB with respect to the mean at all levels below 15 km. This value is slightly less than the 6 dB standard deviation found at the top of the planetary boundary layer (16). As pointed out in the latter paper, a constant standard deviation is important because it reduces the log-normal model for C_n^2 to a one parameter model. Further, we note that the well-behaved nature of the distribution in Figure 6 shows that the shape of the mean vertical profile in Figure 5 is not due to a few wild numbers, but rather is statistically reliable.

Part of the variance at each level implied by the distributions in Figure 6 is likely due to random sampling fluctuations, but part of it can be ascribed to diurnal variations or is associated with synoptic weather changes as discussed next.

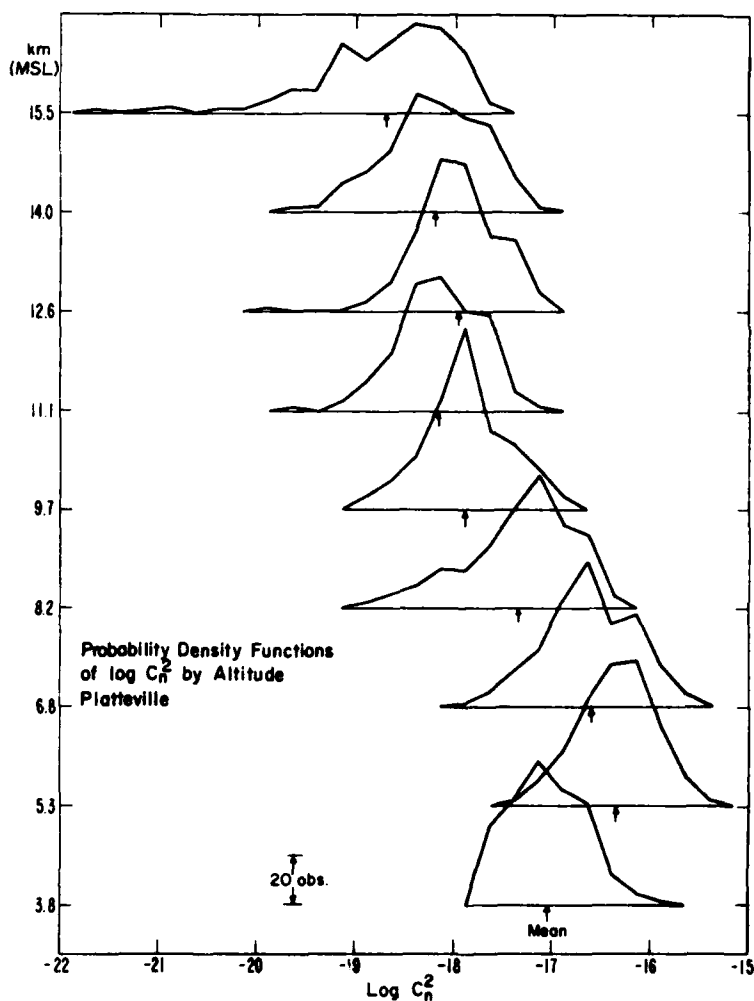


Figure 6. Probability density functions of half-hour averages of C_n^2 by altitude.

In an effort to estimate the diurnal variation of C_n^2 , the data for the same times of day over all days were averaged. To reduce sampling fluctuations, three-hourly averages were used, and the resulting mean curves are given in Figure 7. At mid- and upper-tropospheric heights, a smooth diurnal variation is evident, with maximum average C_n^2 during the afternoon. In the lower stratosphere there seem to be two daily minima separated by two maxima: one in late morning and the other in early evening. These results are summarized in Figure 8 as vertical profiles of the diurnal range and time of maximum of C_n^2 . The range is given in dB, defined as ten times the logarithm of the ratio of the daily maximum to minimum. At stratospheric levels the time of the secondary maximum is also plotted.

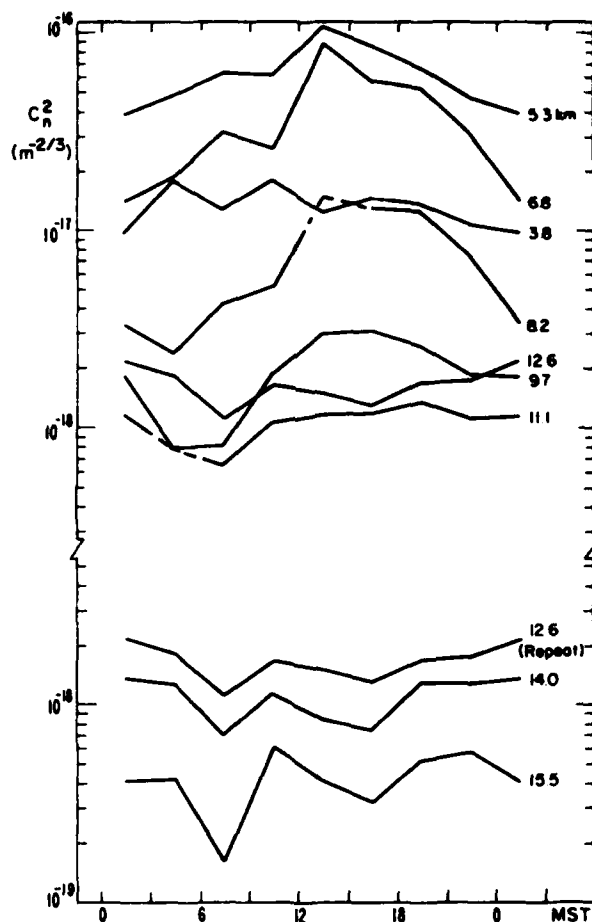


Figure 7. Diurnal variation of C_n^2 at Platteville by altitude.

The large variations among the mean values at different times of the day are expected to contribute to the spread of the distribution functions in Figure 6. This expectation is verified, for example, by the nighttime and afternoon distribution functions in Figure 9. These distributions are not exactly bell shaped, because the number of observations under each curve is small and so sampling fluctuations are relatively large, but the point that combining different hours of the day will broaden the distribution of all data is clear.

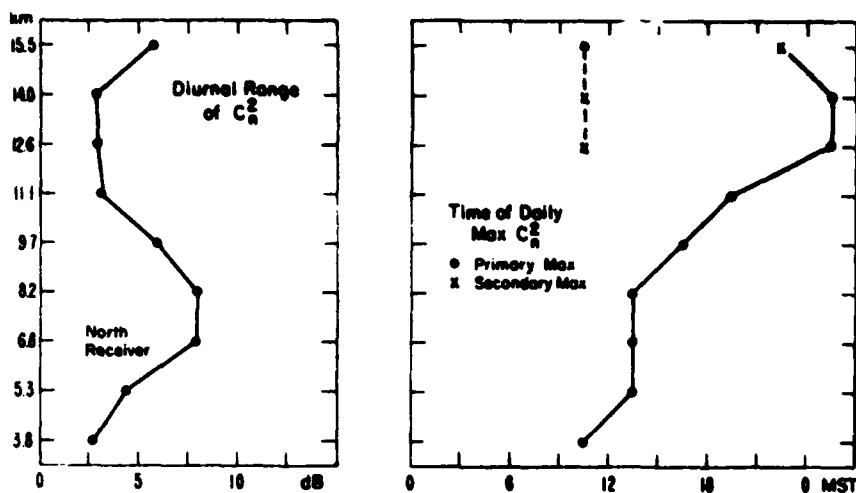


Figure 8. Vertical profiles of diurnal range (max/min) and time of maximum of C_n^2 .

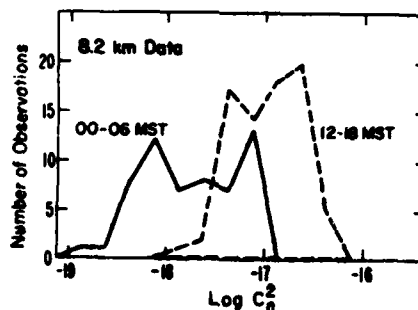


Figure 9. Probability density functions for night- and daytime hours.

Turbulence is more likely near jet streams than in other places. As C_n^2 is a parameter of turbulence, it also should be enhanced in high wind situations. This expectation is verified, for example, by the correlation of the C_n^2 and wind speed data in Figure 10. The correlation coefficient (0.60) is significantly different from zero at the 95% level based on routine a priori tests. Others have noted a correlation between wind speed and C_n^2 in the upper troposphere (15), so this results is not new. However, it confirms the past results and also illustrates that part of the spread of the distribution functions in Figure 6 is due to synoptic weather (wind speed) changes.

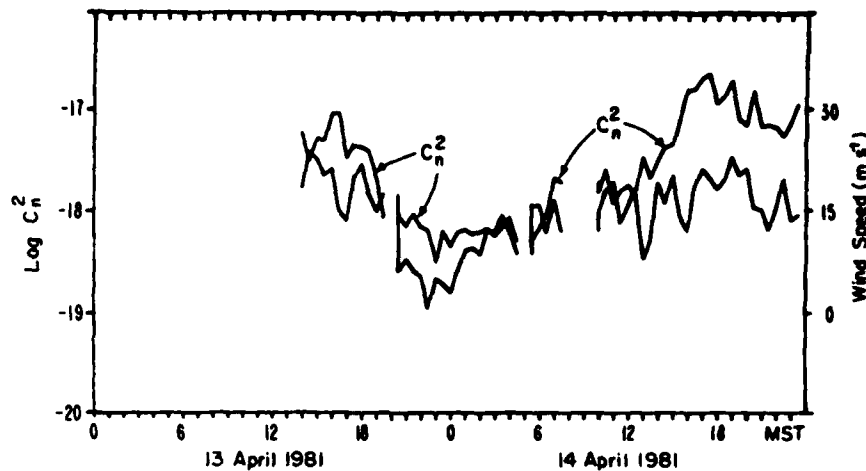


Figure 10. Time series of $\log C_n^2$ and wind speed at 8.2 km. Half-hourly averages. Correlation = 0.60.

5. Summary and Conclusions

The VHF Doppler radar at Platteville is a valuable new tool for meteorological and communications engineering applications. By incorporating high time resolution profiles of the 3-component wind vector along with other meteorological data from the PROFS network, a host of unique studies will be possible. These studies can have immediate practical applications, such as updating forecast model outputs or defining high wind-shear zones, or they can be aimed at theoretical questions such as wave flux calculations or ageostrophic wind development.

The measurements of C_n^2 represent a significant addition to the meager data on C_n^2 variability in the remote troposphere. In fact, Walters and Kunkel (17) bluntly stated that "definitive C_n^2 measurements [above the boundary layer] do not exist". As more ST radar data are collected, definitive climatologies of C_n^2 from about 3-16 km will be possible. One preliminary climatology has already been prepared using data from Poker Flat, Alaska (18). The Platteville results are important because they agree with, and thus support, the Poker Flat data from the same time of year, suggesting that the shape of the vertical profile of C_n^2 , the diurnal variation, or the relationship of C_n^2 with wind speed perhaps can be extrapolated from one location to another.

While these results have been presented in the context of communications engineering, they also have implications for meteorological applications because C_n^2 is directly related to the eddy dissipation rate, ϵ (19). For example, in numerical prediction models ϵ is usually parameterized in terms of the mean wind speed. But C_n^2 is not always closely correlated with wind speed, so this parameterization of ϵ must be an oversimplification. By studying the relation between C_n^2 and wind speed, and perhaps other variables, it will be possible to better parameterize or predict ϵ . Further Trout and Panofsky (20) have shown there is a semi-quantitative relationship between ϵ and turbulence levels as experienced by aircraft. It thus should be possible to use the backscattered power data to directly predict the probability of hazardous turbulence at a given altitude.

The following conclusions have been reached:

1. High time-resolution radar wind observations display much detail, both in horizontal and vertical winds, which go undetected with conventional balloon sounding data.

2. The mean radio refractivity structure constant, C_n^2 , decreases about 2dB/km between about 5 and 15 km. There is a steeper decrease in the upper troposphere and a small increase near the tropopause.
3. C_n^2 has a diurnal variation in the mid- and upper troposphere with daily ranges from 5-8 dB. In the lower stratosphere there seem to be two separate daily maxima of C_n^2 .
4. There is evidence that as wind speed increases C_n^2 increases.

Acknowledgement. Helpful discussions with B. B. Balsley, D. A. Carter, W. L. Ecklund, K. S. Gage, and R. G. Strauch are gratefully acknowledged. Figure 2 and 3 were prepared by the Atmospheric Dynamics Group, Aeronomy Laboratory (NOAA).

References

1. Ecklund, W. L., D. A. Carter, and B. B. Balsley, 1979: Continuous measurement of upper atmospheric winds and turbulence using a VHF Doppler radar: preliminary results. J. Atmos. Terr. Phys., 41, 983-994.
2. Hardy, K. R., 1972: Studies of the clear atmosphere using high power radar. Remote Sensing of the Troposphere, ed. V. E. Derr, Chap. 14, NOAA, Washington, D.C.
3. Balsley, B. B. and K. S. Gage, 1980: The MST radar technique: Potential for middle atmospheric studies. PAGEOPH, 118, 452-493.
4. Balsley, B. B., 1978: The use of sensitive coherent radars to examine atmospheric parameters in the height range 1-100 km. Preprints, 18th Conf. on Radar Meteor. (Atlanta), Am. Meteor. Soc., Boston, pp. 190-193.
5. Gage, K. S., and B. B. Balsley, 1978: Doppler radar probing of the clear atmosphere. Bull. Am. Meteor. Soc., 59, 1074-1093.
6. Van Zandt, T. E., J. L. Green, K. S. Gage, and W. L. Clark, 1978: Vertical profiles of refractivity turbulence structure constant: Comparison of observations by the Sunset radar with a new theoretical model. Radio Sci., 13, 819-829.
7. Ecklund, W. L., K. S. Gage, and B. B. Balsley, 1981: An comparison of vertical wind variations observed with the Platteville VHR radar and local weather conditions. Preprints, 20th Conf. on Radar Meteor. (Boston) Am. Meteor. Soc., Boston, November 30 - December 3.
8. Gage, K. S. and J. L. Green, 1978: Evidence for specular reflection from monostatic VHF radar observations of the stratosphere. Radio Sci., 13, 991-1001.
9. Rottger, J., and C.H. Liu, 1978: Partial reflection and scattering of VHF radar signals from the clear atmosphere. Geophys. Res. Lett., 5, 357-360.
10. Norton, K. A., and J. B. Wisener, 1955: The scatter propagation issue. Proc. of the IRE, 43, 1174.
11. Gossard, E. E., 1977: Refractive index variance and its height distribution in different air masses. Radio Sci., 12, 89-105.
12. Ochs, G. R., T. Wang, R. S. Lawrence, and S. F. Clifford, 1976: Refractive-turbulence profiles measured by one-dimensional filtering of scintillations. Appl. Opt., 15, 2504-2510.
13. Ochs, G. R., and R. S. Lawrence, 1972: Temperature and C_n^2 profiles measured over land and ocean to 3 km above the surface. NOAA TR-ERL 251-MPL 22, NOAA, Washington, DC.
14. Balsley, B. B., and V. L. Peterson, 1981: Doppler-radar measurements of clear air atmospheric turbulence at 1290 MHz. J. Appl. Meteor., 20, 266-274.

15. Hufnagel, R. E., 1974: Variations of atmospheric turbulence. Digest of Technical Papers, Topical Meeting on Optical Propagation through Turbulence. Opt. Soc. of Am., Washington, DC.
16. Chadwick, R. B., and K. P. Morgan, 1980: Long-term measurements of C_n^2 in boundary layer. Radio Sci., 15, 355-361.
17. Walters, D. L., and K. E. Kunkel, 1981: Atmospheric MTF for desert and mountain locations - the atmospheric effects of r_0 . J. Opt. Soc. Am., 71, 397-415.
18. Nastrom, G. D., K. S. Gage, and B. B. Balsley, 1981: The variability of C_n^2 at Poker Flat, Alaska, from MST Doppler radar observations. Opt. Engng., in press.
19. Gage, K. S., J. L. Green, and T. E. Van Zandt, 1980: Use of Doppler radar for the measurement of atmospheric turbulence parameters from the intensity of clear-air echoes. Radio Sci., 15, 407-416.
20. Trout, D. and H. A. Panofsky, 1969: Energy dissipation near the tropopause. Tellus, 21, 355-358.